

# Compositions of MgTiO<sub>3</sub>–CaTiO<sub>3</sub> ceramic with two borosilicate glasses for LTCC technology

Heli Jantunen<sup>a,\*</sup>, Risto Rautioaho<sup>b</sup>, Antti Uusimäki<sup>a</sup>, Seppo Leppävuori<sup>a</sup>

<sup>a</sup>Microelectronics Laboratory and EMPART Research Group of Infotech Oulu, University of Oulu, PO Box 4500, FIN-90014 Oulu, Finland

<sup>b</sup>Materials Engineering Laboratory and EMPART Research Group of Infotech Oulu, University of Oulu, PO Box 4500, FIN-90014 Oulu, Finland

Received 6 January 2000; received in revised form 20 April 2000; accepted 29 April 2000

## Abstract

Mixtures of ZnO–SiO<sub>2</sub>–B<sub>2</sub>O<sub>3</sub>/MgTiO<sub>3</sub>–CaTiO<sub>3</sub> (ZSB/MMT-20) and BaO–SiO<sub>2</sub>–B<sub>2</sub>O<sub>3</sub>/MgTiO<sub>3</sub>–CaTiO<sub>3</sub> (BSB/MMT-20) have been investigated as new candidates for LTCC dielectric materials. Two-stage sintering behaviour was observed in both materials, starting at around 600 and 850°C. Nearly full density (97%) was achieved in ZSB/MMT-20 after sintering at 900°C, while a high porosity of 23% was measured in BSB/MMT-20 after firing at 875°C followed by partial melting of samples during sintering at 900°C. After firing, fully crystalline structure with phases of ZnTiO<sub>3</sub>, Zn<sub>2</sub>SiO<sub>4</sub>, Mg<sub>4/3</sub>Zn<sub>2/3</sub>B<sub>2</sub>O<sub>5</sub> and TiO<sub>2</sub> were found in ZSB/MMT-20, while the structure of BSB/MMT-20 consisted of crystalline TiO<sub>2</sub> and BaTi(BO<sub>3</sub>)<sub>2</sub> and amorphous SiBa(BO<sub>3</sub>)<sub>2</sub> and SiB<sub>2</sub>O<sub>5</sub>. ZSB/MMT-20 fired at 900°C showed promising microwave properties having the dissipation factor of 0.001 and a permittivity of 10.6 at 7 GHz. The corresponding values for BSB/MMT-20 fired at 875°C were 0.002 and 8.2, respectively. © 2000 Elsevier Science Ltd. All rights reserved.

**Keywords:** Dielectric properties; Glass ceramics; MgTiO<sub>3</sub>–CaTiO<sub>3</sub>; Sintering; Substrates

## 1. Introduction

In producing miniaturised devices, ceramic multilayer structures with low sintering temperatures are needed because they can be co-fired with high conductivity, that is low-loss conductors.<sup>1</sup> Low temperature co-fired ceramic (LTCC) technology offers significant benefits over other established packaging technologies for high density, high RF and fast digital applications requiring hermetical packaging and good thermal management.<sup>2</sup> Many new ceramic/glass compositions have recently been developed for microwave purposes, especially low permittivity ( $\epsilon_r$ ) materials using alumina and suitable glass combinations,<sup>3</sup> but also higher  $\epsilon_r$  (20–100) materials.<sup>1,4,5</sup> Table 1 shows the permittivity and dissipation factors (DF) of some currently available commercial LTCC materials.

There are two approaches to exploiting glasses to achieve ceramic compositions sinterable below 1000°C.

The first consists in adding a low softening temperature glass to the crystalline ceramic component (liquid phase sintering); the second is the ‘glass-ceramic’ approach in which the sole starting component is a glass which crystallises during firing.<sup>6</sup> As compared with liquid phase sintering in which the glass phase remains, the advantages offered by the ‘glass-ceramic’ approach include shape stability during the sintering stage, improved dielectric properties and mechanical strength and controlled thermal expansivity.<sup>6,7</sup>

The basic microwave requirements for RF applications are low dissipation factor, DF, (or high  $Q$ -value), optimum values of permittivity,  $\epsilon_r$ , and temperature coefficient of resonant frequency,  $\tau_f$ , all defined by applicational specifications. The sintering temperature should lie between 850 and 950°C for co-firing with high conductivity metals. Although some commercial LTCC compositions are available as shown in Table 1, new low loss dielectric materials are needed especially for high frequency RF applications.

MgTiO<sub>3</sub>–CaTiO<sub>3</sub> ceramic is a well-known dielectric material for microwave applications.<sup>8,9</sup> It combines a

\* Corresponding author.

E-mail address: heja@ee.oulu.fi (H. Jantunen).

Table 1  
Dielectric properties of commercial LTCC materials<sup>a</sup>

	DuPont 951	Ferro A6-5-M-13	Heraeus CT 700
Permittivity (1 MHz)	7.8	5.9	7.0
DF (1 KHz)	0.0015	0.002	0.002
	(1 KHz)	(10 MHz)	(1 kHz)

<sup>a</sup> Data from LTCC Design Guide made by CTS Microelectronics, West Lafayette, IN, USA.

high quality factor  $Q$  (3000–4600 at 6 GHz), low  $\epsilon_r$  (18–20) and the ability to adjust  $\tau_f$  (–10 to +10 ppm K<sup>–1</sup>);<sup>8</sup> it can be utilised in antennas, high-performance substrates, microwave filters and resonators. The only disadvantage of this material is its high sintering temperature (about 1360°C) which, as it stands, is unsuited to LTCC technology. Despite this, in this research the MgTiO<sub>3</sub>–CaTiO<sub>3</sub> compound is selected as a basic dielectric material because of its excellent RF.

In the work reported here two different glass/MgTiO<sub>3</sub>–CaTiO<sub>3</sub> ceramic mixtures have been investigated as new ceramic materials for telecommunication purposes utilising LTCC technology. The minimum microwave properties aspired here were those of currently available commercial LTCC material in Table 1. Sintering behaviour, microstructural and microwave properties of the materials were studied. The aim of the research was to identify compositions sinterable at temperatures below 1000°C and thus compatible with pattern layers of the high conductivity metals necessary to achieve the best microwave performance.

## 2. Experimental procedure

### 2.1. Glass preparation

After testing several different borosilicate glasses, two compositions were chosen to lower the firing temperature of the MgTiO<sub>3</sub>–CaTiO<sub>3</sub>. The first one, 60.3 ZnO–27.1 B<sub>2</sub>O<sub>3</sub>–12.6 SiO<sub>2</sub> (labelled ZSB), was similar to that used by M. Abe et al.<sup>5</sup> with high permittivity BaTiO<sub>3</sub> ceramics. The other glass (labelled BSB) had the eutectic composition, 35 BaO–55 B<sub>2</sub>O<sub>3</sub>–10 SiO<sub>2</sub>.<sup>10</sup> The raw materials used were SiO<sub>2</sub> (99.5% purity), ZnO (99% purity), B<sub>2</sub>O<sub>3</sub> (99.9% purity) from Johnson Matthey GmbH, Germany, and BaO (98% purity) from Fluka Chemie AG, Switzerland.

The glasses were produced by weighing the starting materials and mixing them for 1 h in a polyethylene pot mill using agate balls. The mixed powders were pressed into pellets, which were melted in a platinum crucible at 980°C for 1 h. The melts were quenched into water and

pulverised in the ball mill for 12 h, dried and screened through a 100 mesh sieve.

The specific surface areas of the powders were measured using a BET analyser (OmniSorb 360CX, Coulter Electronics Inc., Ltd., Luton, UK) and their structures by XRD (Siemens D5000, Karlsruhe, Germany) utilising the JCPDS data file (International Center for Diffraction Data 1992, Swarthmore, PA, USA).

### 2.2. Glass/MMT-20 mixture and test sample preparation

The starting dielectric material was commercial MgTiO<sub>3</sub>–CaTiO<sub>3</sub> powder (coded by Fuji Titanium Industry Co., Ltd as MMT-20). Its specific surface area was measured using the BET analyser. The mixtures were produced by weighing appropriate amounts of glasses and ceramic, mixing them in the ball-mill for 2 h together with PVA as a binder, PEG as a plasticiser and distilled water. The compositions were dried in a microwave oven and sieved. Uniaxial pressing at 60 MPa resulted in 18 mm long cylindrical compacts of 12.2 mm diameter for dilatometric studies (Orton Automatic Recording Dilatometer, Westerville, OH, USA) and in 5–10 mm long cylindrical compacts of 25.5 mm diameter for XRD, SEM/EDS (Jeol JSM-640, Tokyo, Japan), FESEM (Jeol JSM-6300F, Tokyo, Japan), density, shrinkage and microwave property studies.

Pure MMT-20 samples (fired at 1360°C) and samples of commercial LTCC-material (fired at 875°C) were also prepared in a similar way for the measurement of  $\epsilon_r$  and  $Q$ -values. The commercial LTCC powder was derived from 'green' sheet material (duPont green tape code 951)<sup>3</sup> following binder burn-out. This powder was granulated in isopropanol as mentioned earlier.

The optimum glass/MgTiO<sub>3</sub>–CaTiO<sub>3</sub> ceramic ratio required for low temperature firing was determined using dilatometry. The densities and shrinkages of the samples were calculated from their dimensions and weights following the various firings. The porosity of the samples was estimated from the SEM images using the line intercept method.

XRD was used to identify crystalline phases. Microstructural and phase analysis was done using SEM/EDS on ground and polished surfaces. Boron contents were derived by the difference between the total determined constituents and 100%.

The dielectric characteristics in the microwave frequency range were measured by the Hakki–Coleman dielectric resonator method, where a cylindrically shaped specimen is positioned between two copper plates.<sup>11</sup> An HP8719C network analyser was used for the microwave measuring system. The dielectric properties were calculated from the frequency of the TE<sub>011</sub> resonant mode.

### 3. Results and discussion

The specific surface areas of the MMT-20 powder and the ZSB and BSB powders were 4.1, 2.6 and 2.4 m<sup>2</sup> g<sup>-1</sup>, respectively.

After several sintering experiments it was concluded that 70 wt.% glass phase in the ceramic was needed to lower the effective firing temperature to the desired 900°C. Fig. 1 shows shrinkage data for three mixtures, demonstrating an interesting, two-stage densification behaviour starting respectively at around 600 and 850°C. The SEM/EDS and XRD data for the materials in the as-mixed and dried condition, and after firing at 620, 875 and 900°C are summarised in Table 2. The as-received MMT-20 powder was composed of MgTiO<sub>3</sub> grains with a very small amount (about 6 mol%) of separate CaTiO<sub>3</sub> grains; the CaTiO<sub>3</sub> could not be detected by XRD in the prepared glass/MMT-20 mixtures. The BSB was totally amorphous, but the ZSB had also crystallised Zn<sub>2</sub>SiO<sub>4</sub>. The compact densities of both mixtures before firing were 1.9 Mg m<sup>-3</sup>.

#### 3.1. BSB/MMT-20 mixture

In the first firing step (620°C, dwell time 10 min) of this mixture, the glass started to sinter causing slight shrinkage. The only crystalline phase observed by XRD (Fig. 2) was MgTiO<sub>3</sub>. The densities of the samples were 2.0 Mg m<sup>-3</sup>.

After the second firing step (875°C, 80 min), the microstructure of the composition consisted of needle-like BaTi(BO<sub>3</sub>)<sub>2</sub> crystals and precipitated TiO<sub>2</sub> crystals surrounded by amorphous SiB<sub>2</sub>O<sub>5</sub> and SiBa(BO<sub>3</sub>)<sub>2</sub>

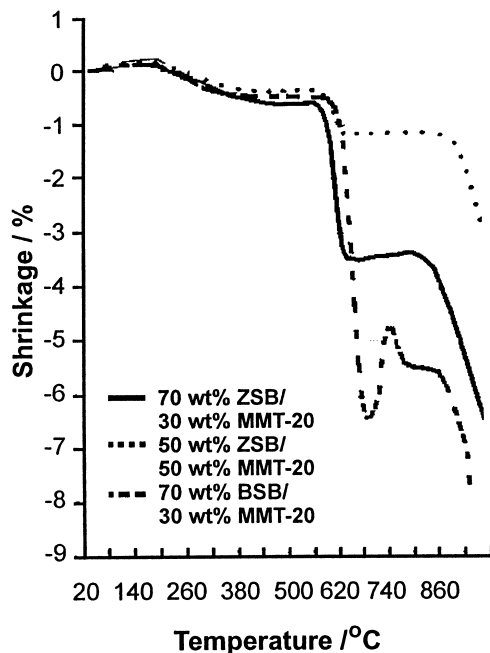


Fig. 1. Shrinkage behaviour of different compositions.

phases. The original MgTiO<sub>3</sub> phase had disappeared. These observations are deduced from an examination of Figs. 2 and 3 taken together.

The density had increased to 2.8 Mg m<sup>-3</sup> with linear shrinkage about 12% and the porosity of the samples was still quite high (about 23 vol.%). After each firing, the microstructure was found to be uniform. After the last firing step (900°C, 80 min), the samples started to lose their shape, and at 920°C they were totally molten.

#### 3.2. ZSB/MMT-20 mixture

After firing at 620°C, the microstructure contained densified areas, where glass had started to react with the crystalline material producing different amorphous and crystalline phases composed of the original glass

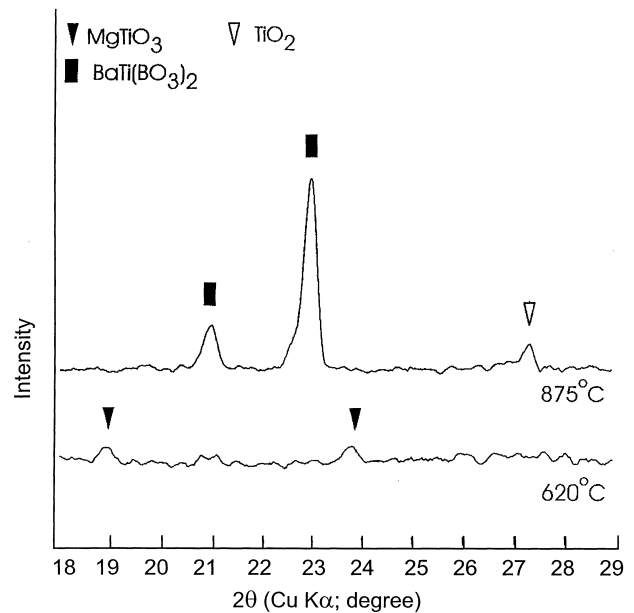


Fig. 2. XRD patterns of BSB/MMT-20 mixture.

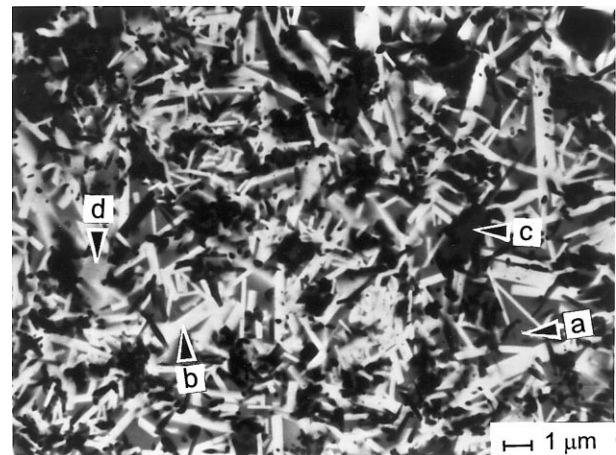


Fig. 3. SEM/BE image of BSB/MMT-20 mixture after 875°C firing. (a) TiO<sub>2</sub> crystal, (b) BaTi(BO<sub>3</sub>)<sub>2</sub> crystal and amorphous (c) SiB<sub>2</sub>O<sub>5</sub> and (d) SiBa(BO<sub>3</sub>)<sub>2</sub>.

Table 2  
Densities and SEM/EDS and XRD results for the samples after various process steps

Sample	Compacts before firing	After firing at 620°C for 10 min	After firing at 875°C for 80 min	After firing at 900°C for 80 min
MMT-20	Crystalline MgTiO <sub>3</sub> , CaTiO <sub>3</sub>			
BSB	Totally amorphous			
ZSB	Glass and crystalline Zn <sub>2</sub> SiO <sub>4</sub>			
BSB/MMT-20 mixture (70 wt.%/30 wt.%)		Crystalline MgTiO <sub>3</sub> and amorphous SiBa(BO <sub>3</sub> ) <sub>2</sub> and Ba <sub>2</sub> B <sub>6</sub> O <sub>11</sub>	Crystalline TiO <sub>2</sub> , BaTi(BO <sub>3</sub> ) <sub>2</sub> and amorphous SiBa(BO <sub>3</sub> ) <sub>2</sub> and SiB <sub>2</sub> O <sub>5</sub>	–
Density/Mg m <sup>-3</sup> (Porosity vol.%)	1.9 (47)	2.0 (44)	2.8 (23)	
ZSB/MMT-20 mixture (70 wt.%/30 wt.%)		Crystalline ZnSiO <sub>4</sub> , MgTiO <sub>3</sub> and amorphous 54ZnO + 9SiO <sub>2</sub> + 37B <sub>2</sub> O <sub>3</sub> , ZnO + 3TiO <sub>2</sub> + 6B <sub>2</sub> O <sub>3</sub> and 35CaO + 41TiO <sub>2</sub> + 6ZnO + 18B <sub>2</sub> O <sub>3</sub>	Crystalline ZnTiO <sub>3</sub> , Zn <sub>2</sub> SiO <sub>4</sub> , Mg <sub>2</sub> ZnTi(BO <sub>3</sub> ) <sub>2</sub> O <sub>2</sub> , TiO <sub>2</sub> and no amorphous phases found	Crystalline ZnTiO <sub>3</sub> , Zn <sub>2</sub> SiO <sub>4</sub> , Mg <sub>4/3</sub> Zn <sub>2/3</sub> B <sub>2</sub> O <sub>5</sub> , TiO <sub>2</sub> and no amorphous phases found
Density/Mg m <sup>-3</sup> (Porosity vol.%)	1.9 (47)	2.2 (39)	3.1 (14)	3.5 (3.5)

material, together with titanium and calcium. The original MgTiO<sub>3</sub> crystals and the original Zn<sub>2</sub>SiO<sub>4</sub> crystals could also easily be observed in XRD (Fig. 4). The sample density values were 2.2 Mg m<sup>-3</sup>.

In the second step (875°C), no amorphous phases could be found and the density of the samples was 3.1

Mg m<sup>-3</sup>. The microstructural variation was still present (Fig. 5) showing uniform, matrix-like areas and large areas, (even > 100 μm diameter), in which the inner parts were composed of the original crystalline material and MgO–TiO<sub>2</sub>–B<sub>2</sub>O<sub>3</sub> crystals, and the outer areas contained ZnTiO<sub>3</sub>, Mg<sub>2</sub>ZnTi(BO<sub>3</sub>)<sub>2</sub>O<sub>2</sub> and TiO<sub>2</sub> crystals. The matrix-like uniform area consisted mainly of Zn<sub>2</sub>SiO<sub>4</sub> and Mg<sub>2</sub>ZnTi(BO<sub>3</sub>)<sub>2</sub>O<sub>2</sub> crystals. All these phases were positively identified by XRD (Fig. 4), except

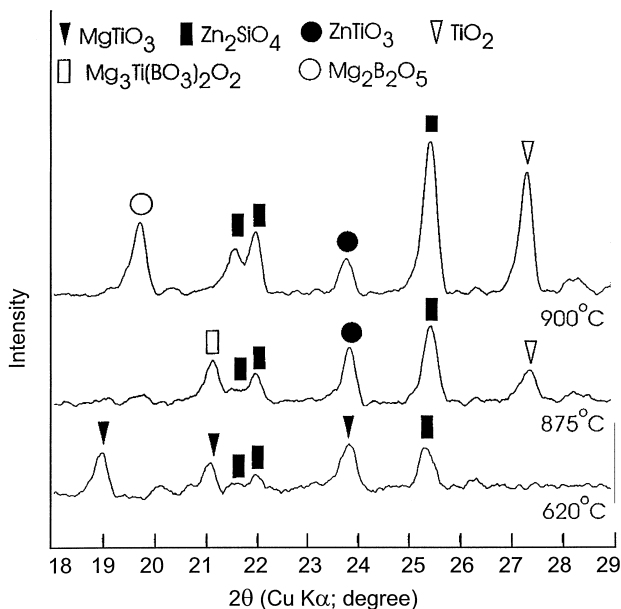


Fig. 4. XRD patterns of ZSB/MMT-20 mixture.

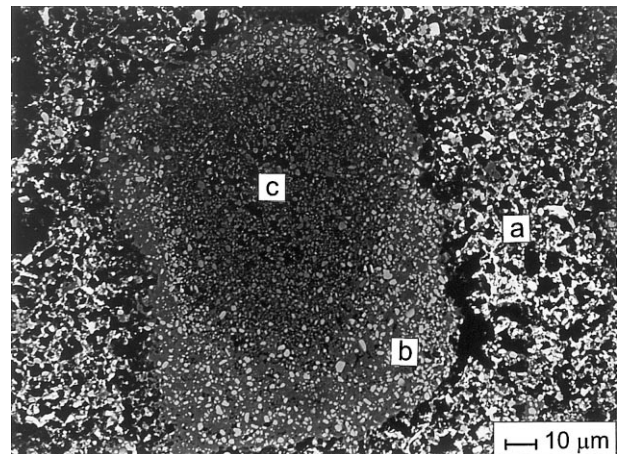


Fig. 5. SEM/BE image of the ZSB/MMT-20 mixture after firing at 875°C. (a) Crystalline Zn<sub>2</sub>SiO<sub>4</sub> and Mg<sub>2</sub>ZnTi(BO<sub>3</sub>)<sub>2</sub>O<sub>2</sub>; (b) crystalline ZnTiO<sub>3</sub> and Mg<sub>2</sub>ZnTi(BO<sub>3</sub>)<sub>2</sub>O<sub>2</sub>; (c) MgTiO<sub>3</sub>, CaTiO<sub>3</sub>, CaTiO<sub>3</sub> and mixtures of MgO–TiO<sub>2</sub>–B<sub>2</sub>O<sub>3</sub> crystals.

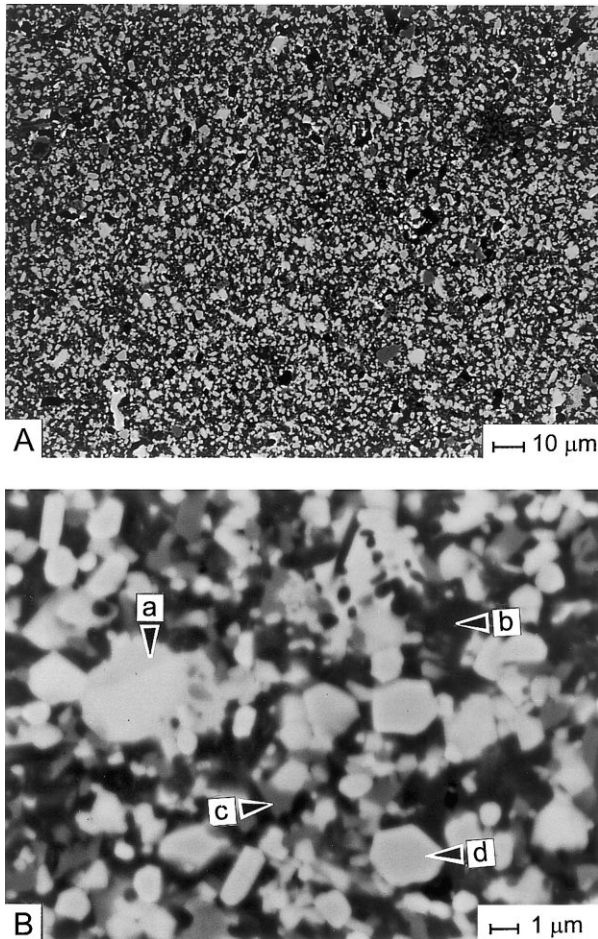


Fig. 6. (A). SEM/BE and (B) FESEM/BE images of the ZSB/MMT-20 mixture after firing at 900°C. (a)  $\text{Zn}_2\text{SiO}_4$ ; (b)  $\text{Mg}_{4/3}\text{Zn}_{2/3}\text{B}_2\text{O}_5$ ; (c)  $\text{TiO}_2$  (with 5–6 wt.% ZnO); (d)  $\text{ZnTiO}_3$ .

for  $\text{Mg}_2\text{ZnTi}(\text{BO}_3)_2\text{O}_2$  the presence of which was inferred from the JCPDS file for  $\text{Mg}_3\text{Ti}(\text{BO}_3)_2\text{O}_2$ . According to the EDS analyses, the  $\text{TiO}_2$  crystals contained about 5–6 wt.% ZnO.

After the 900°C firing step, the large scale microstructural variation totally disappeared (Fig. 6A) and the material consisted of crystals smaller than 5 μm in size with no amorphous phases (Fig. 6B). Compared to

the earlier step, the  $\text{ZnTiO}_3$  and  $\text{Zn}_2\text{SiO}_4$  crystals were still present and the amount of  $\text{TiO}_2$  crystalline phase had increased as well as  $\text{Zn}_2\text{SiO}_4$ . A tentative explanation is that  $\text{Mg}_2\text{ZnTi}(\text{BO}_3)_2\text{O}_2$  decomposed mainly to  $\text{TiO}_2$  and  $\text{Mg}_{4/3}\text{Zn}_{2/3}\text{B}_2\text{O}_5$ , which was inferred from the JCPDS file for  $\text{Mg}_2\text{B}_2\text{O}_5$ . This explanation is based on the XRD analysis evidence for the presence of  $\text{Mg}_2\text{B}_2\text{O}_5$  (Fig. 4) after firing at 900°C but absent earlier. The density of the samples was  $3.5 \text{ Mg m}^{-3}$  with linear shrinkage about 20%.

### 3.3. Dielectric properties

The dielectric properties were measured at approximately 7 GHz except for the MMT-20 samples, and for the commercial LTCC samples where the frequency was 6 GHz. The results are given in Table 3.

Although the amounts of glass in both mixtures required to decrease the firing temperature from 1360 to 900°C were large, the electrical properties were promising compared to those of the commercial LTCC material. When other comparing the effectiveness of the ZSB and BSB additions to MMT-20 ceramic the former is the more promising since it produced nearly fully dense and crystalline material. This composition also had higher permittivity and lower dissipation factor, both parameters improving the higher the firing temperature and the attendant increasing  $\text{TiO}_2$  crystalline phase.

Generally speaking, because of differences in specimen geometries and measuring systems, dielectric properties reported in different studies are difficult to compare.<sup>1,3–5</sup> In spite of this, although the glass addition decreased the permittivity and the increased DF from the values for the pure MMT-20 ceramic, the modified materials are competitive with materials having similar glass content<sup>1,5</sup> and with the commercial ones in Table 1. The firing temperature is still slightly too high, but a minor change in glass composition could remedy this. In future, it might prove possible to even lower the glass addition, which should improve microwave properties bringing them closer to those of the original MMT-20 ceramic. Also, in the case of BSB glass addition, combinations of BaO,  $\text{SiO}_2$  and  $\text{B}_2\text{O}_3$  are possible<sup>10</sup> and these might lead to a totally crystalline structure and improved microwave properties.

The study is a preliminary investigation of these mixtures and will be continued with profound measurements of thermomechanical, microstructural and microwave properties of at least the ZSB/MMT-20 mixture.

## 4. Conclusions

The BSB/MMT-20 and ZSB/MMT-20 mixtures showed two shrinkage behaviours, the first one starting

Table 3  
Measured dielectric properties

Sample	Permittivity	Q-value	DF × 10 <sup>-3</sup>
MMT-20, fired 1360°C	21.4	3700	0.3
BSB/MMT-20 mixture, fired 875°C	8.2	430	2.3
ZSB/MMT-20 mixture, fired 875°C	8.5	830	1.2
ZSB/MMT-20 mixture, fired 900°C	10.6	880	1.1
Commercial LTCC, fired 875°C	7.4	320	3.1

near 600°C and the second one near 850°C. In the case of the BSB/MMT-20 composition, the first stage shrinkage is caused by the onset of liquid phase sintering. The final state of this composition consisted of amorphous  $\text{SiB}_2\text{O}_5$  and  $\text{SiBa}(\text{BO}_3)_2$  phases, crystalline  $\text{TiO}_2$  and needle-like  $\text{BaTi}(\text{BO}_3)_2$  phases. Although this composition did not reach the full density (porosity about 23%) before melting, its DF was still lower (0.002 at 7 MHz) than that measured for the commercial LTCC material (0.003 at 6 GHz), while values for the permittivity (8–9) were rather similar. This composition did not reach the intended totally crystalline structure.

The first stage shrinkage of the ZSB/MMT-20 composition evidenced the onset of liquid phase sintering coupled with solution-precipitation reactions. At higher temperatures (875°C), all amorphous phases had vanished and the microstructure was composed of crystalline  $\text{Zn}_2\text{SiO}_4$ ,  $\text{TiO}_2$ ,  $\text{ZnTiO}_3$  and  $\text{Mg}_2\text{ZnTi}(\text{BO}_3)_2\text{O}_2$  phases. In a firing at 900°C, the  $\text{Mg}_2\text{ZnTi}(\text{BO}_3)_2\text{O}_2$  phase seemed to decompose to  $\text{Mg}_{4/3}\text{Zn}_{2/3}\text{B}_2\text{O}_5$  and  $\text{TiO}_2$  phases and the samples had low porosity (3.5%). The microwave properties also changed showing higher permittivity ( $\epsilon_r = 10.6$ ) and low DF (0.001 at 7 GHz), observations which were consistent with the microstructural development.

### Acknowledgements

The study is supported by the Academy of Finland (project 163324).

### References

1. Takada, T., Wang, S. F., Yoshikawa, S., Jang, S.-J. and Newnham, R. E., Effects of glass additions on  $(\text{Zr},\text{Sn})\text{TiO}_4$  for microwave applications. *J. Am. Ceram. Soc.*, 1994, **77**, 2485–2488.
2. Scramton, C. Q. and Lawson, J. C., LTCC technology: where we are and where we're going-II. In *IEEE Symposium on Technologies for Wireless Applications* 1999, pp. 193–200.
3. Donohue, P. C., Taylor, B. E., Amey, D. I., Draudt, R. R., Smith, M. A., Horowitz, S. J. and Larry, J. R., A new low loss lead free LTCC system for wireless and RF applications. In *1998 International Conference on Multichip Modules and High Density Packaging*, IEEE 1998, pp. 196–199.
4. Kniajer, G., Dechant, K. and Apté, P., Low loss, low temperature cofired ceramics with higher dielectric constants for multichip modules (MCM). In *1997 International Conference on Multichip Modules*, IEEE, 1997, pp. 121–127.
5. Abe, M., Nanataki, T. and Yano, S., Dielectric ceramic composition containing  $\text{ZnO-B}_2\text{O}_3\text{-SiO}_2$  glass, method of preparing the same, and resonator and filter using the dielectric ceramic composition. *US Patent* 5,493,262, 20 February 1996.
6. Knickerbocker, S. H., Kumar, A. H. and Herron, L. W., Cordierite glass-ceramics for multilayer ceramic packaging. *Am. Ceram. Bull.*, 1993, **72**, 90–95.
7. McMillan, P. W., *Glass Ceramics*, Academic Press, London, 1979, pp. 208–209.
8. Katoh, T. and Ozeki, H., Microwave dielectric ceramic composition. *US Patent* 5,340,784, 23 August 1994.
9. Wood, D. C., Lee, H. Y., Kim, J.-J., Kim, T.-H., Lee, S.-J., Park, J.-R. and Choy, T. G., Microwave dielectric properties of doped- $\text{MgTiO}_3$  ceramics. In *Proceedings of the Tenth IEEE International Symposium on Applications of Ferroelectrics*, IEEE, 1996, pp. 863–866.
10. Levin, E. M., Robbins, C. R. and McMurdie, H. F., *Phase Diagrams for Ceramists*, ed. M. K. Reser. American Ceramic Society, Columbus, OH, 1964, Fig. 561.
11. Hakki, B. W. and Coleman, P. D., A dielectric resonator method of measuring inductive capacities in the millimeter range. *IRE Trans. Microwave Theory Tech.*, 1960, **MTT8**, 402–410.